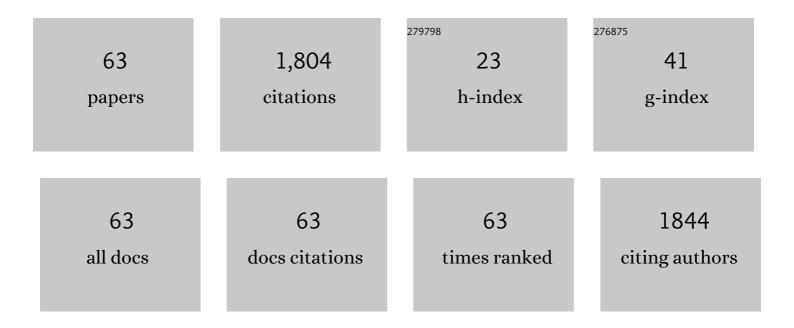
List of Publications by Year in descending order

Source: https://exaly.com/author-pdf/2904164/publications.pdf Version: 2024-02-01



#	Article	IF	CITATIONS
1	Silver Nanowires with Ultrabroadband Plasmon Response for Ultrashort Pulse Fiber Lasers. Advanced Photonics Research, 2022, 3, .	3.6	6
2	25.8 W All-Fiber Mid-Infrared Supercontinuum Light Sources Based on Fluorotellurite Fibers. IEEE Photonics Technology Letters, 2022, 34, 367-370.	2.5	10
3	Cascaded Raman amplifiers based on fluorotellurite fibers. Optical Materials Express, 2022, 12, 2309.	3.0	2
4	Design of a Few-Mode Erbium-Ytterbium Co-Doped Polymer Optical Waveguide Amplifier With Low Differential Modal Gain. Journal of Lightwave Technology, 2021, 39, 3201-3216.	4.6	12
5	Intense emission at â^¼3.3  µm from Er <sup>3+</sup> -doped fluoroindate glass fiber. Optics Letters, 2 46, 1057.	2 <u>021</u> , 3.3	22
6	Unlocking the ultrafast potential of gold nanowires for mode-locking in the mid-infrared region. Optics Letters, 2021, 46, 1562.	3.3	21
7	Triangular gold nanoplates as saturable absorber for passively Q-switched fiber laser at 1.56 μm. Laser Physics Letters, 2021, 18, 095101.	1.4	3
8	Sapphire-Derived Fiber Bragg Gratings for High Temperature Sensing. Crystals, 2021, 11, 946.	2.2	6
9	Ceriumâ€Doped Perovskite Nanocrystals for Extremely Highâ€Performance Deepâ€Ultraviolet Photoelectric Detection. Advanced Optical Materials, 2021, 9, 2100423.	7.3	12
10	Efficient â^¼4  µm emission from Pr <sup>3+</sup> /Yb <sup>3+</sup> co-doped fluoroindate glass. Op Letters, 2021, 46, 5607.	otics 3.3	14
11	MnO <sub>2</sub> nanosheets as saturable absorbers for a Q-switched fiber laser. Optical Materials Express, 2020, 10, 3097.	3.0	7
12	Single-Frequency kHz-Linewidth 1070 nm Laser Based on Yb:YAG Derived Silica Fiber. IEEE Photonics Technology Letters, 2020, 32, 895-898.	2.5	8
13	Semiconducting polymer dots as broadband saturable absorbers for Q-switched fiber lasers. Journal of Materials Chemistry C, 2020, 8, 4919-4925.	5.5	23
14	Passively Mode-Locked Operations Induced by Semiconducting Polymer Nanoparticles and a Side-Polished Fiber. ACS Applied Materials & amp; Interfaces, 2020, 12, 57461-57467.	8.0	25
15	22.7  W mid-infrared supercontinuum generation in fluorotellurite fibers. Optics Letters, 2020, 45, 1882	. 3.3	30
16	Ho <sup>3+</sup> /Pr <sup>3+</sup> Co-Doped AlF <sub>3</sub> Based Glass Fibers for Efficient ~2.9 <i>μ</i> m Lasers. IEEE Photonics Technology Letters, 2020, 32, 1489-1492.	2.5	6
17	Linearly polarized single-frequency fiber laser based on the Yb:YAG-crystal derived silica fiber. Applied Optics, 2020, 59, 9931.	1.8	5
18	Green/red pulsed vortex-beam oscillations in all-fiber lasers with visible-resonance gold nanorods. Nanoscale, 2019, 11, 15991-16000.	5.6	19

#	Article	IF	CITATIONS
19	Broadband supercontinuum generation from 600 to 5400 nm in a tapered fluorotellurite fiber pumped by a 2010 nm femtosecond fiber laser. Applied Physics Letters, 2019, 115, 091103.	3.3	9
20	Wideband Tunable, Carbon Nanotube Mode-Locked Fiber Laser Emitting at Wavelengths Around \$3~mu\$ m. IEEE Photonics Technology Letters, 2019, 31, 869-872.	2.5	8
21	KMnF3:Yb3+,Er3+ Core-Active-Shell Nanoparticles with Broadband Down-Shifting Luminescence at 1.5 μm for Polymer-Based Waveguide Amplifiers. Nanomaterials, 2019, 9, 463.	4.1	9
22	Mesoporous carbon nanospheres deposited onto D-shaped fibers for femtosecond pulse generation. RSC Advances, 2019, 9, 11621-11626.	3.6	10
23	Mid-Infrared Q-Switched and Mode-Locked Fiber Lasers at 2.87 <italic>μ</italic> m Based on Carbon Nanotube. IEEE Journal of Selected Topics in Quantum Electronics, 2019, 25, 1-6.	2.9	18
24	Nearâ€Infrared Broadband Polymerâ€Dot Modulator with High Optical Nonlinearity for Ultrafast Pulsed Lasers. Laser and Photonics Reviews, 2019, 13, 1800326.	8.7	28
25	All-fiber-integrated Yb:YAG-derived silica fiber laser generating 6 W output power. Optics Express, 2019, 27, 3791.	3.4	26
26	Large aspect ratio gold nanorods (LAR-GNRs) for mid-infrared pulse generation with a tunable wavelength near 3 1¼m. Optics Express, 2019, 27, 4886.	3.4	32
27	Gold nanowires with surface plasmon resonance as saturable absorbers for passively Q-switched fiber lasers at 2 µm. Optical Materials Express, 2019, 9, 2406.	3.0	21
28	Q-switched lasing at the 2 µm wavelength induced by Cu <sub>18</sub> S nanocrystals. OSA Continuum, 2019, 2, 2809.	1.8	4
29	Design of Fluorotellurite Microstructured Fibers With Near-Zero-Flattened Dispersion Profiles for Optical-Frequency Comb Generation. Journal of Lightwave Technology, 2018, 36, 2211-2215.	4.6	7
30	Amplification of wavelength-shifting soliton in active photonic crystal fibers. Applied Physics Letters, 2018, 112, 161105.	3.3	1
31	2875 nm Lasing From Ho <sup>3+</sup> -Doped Fluoroindate Glass Fibers. IEEE Photonics Technology Letters, 2018, 30, 323-326.	2.5	27
32	Fluorotellurite Microstructured Fibers and Their Applications. , 2018, , .		0
33	Tunable mid-infrared Raman soliton generation from 1.96 to 2.82 μm in an all-solid fluorotellurite fiber. AIP Advances, 2018, 8, .	1.3	23
34	Stable Dissipative Soliton Generation From Yb-Doped Fiber Laser Modulated via Evanescent Field Interaction With Gold Nanorods. IEEE Photonics Journal, 2018, 10, 1-8.	2.0	4
35	Mesoporous Carbon Nanospheres as Broadband Saturable Absorbers for Pulsed Laser Generation. Advanced Optical Materials, 2018, 6, 1800606.	7.3	23
36	High-power mid-infrared supercontinuum laser source using fluorotellurite fiber. Optica, 2018, 5, 1264.	9.3	85

#	Article	IF	CITATIONS
37	Coherent supercontinuum generation from 1.4 to 4 <i>μ </i> m in a tapered fluorotellurite microstructured fiber pumped by a 1980 nm femtosecond fiber laser. Applied Physics Letters, 2017, 110, .	3.3	26
38	Plasmonic Cu <sub>1.8</sub> S nanocrystals as saturable absorbers for passively Q-switched erbium-doped fiber lasers. Journal of Materials Chemistry C, 2017, 5, 4034-4039.	5.5	31
39	Gold nanorods saturable absorber for Q-switched Nd:GAGG lasers at 1Âμm. Applied Physics B: Lasers and Optics, 2017, 123, 1.	2.2	10
40	Enhancement of phase-matched third harmonic generation via soliton self-frequency shift cancellation in a fluorotellurite microstructured fiber. Applied Physics Letters, 2017, 111, 151103.	3.3	1
41	4.5 W supercontinuum generation from 1017 to 3438 nm in an all-solid fluorotellurite fiber. Applied Physics Letters, 2017, 110, 261106.	3.3	13
42	Dual-wavelength mode-locked thulium-doped fiber laser based on carbon nanotube. , 2016, , .		0
43	Tunable dual-wavelength passively mode-locked thulium-doped fiber laser using carbon nanotube. Optical Engineering, 2016, 55, 106115.	1.0	12
44	Local Field Modulation Induced Threeâ€Order Upconversion Enhancement: Combining Surface Plasmon Effect and Photonic Crystal Effect. Advanced Materials, 2016, 28, 2518-2525.	21.0	240
45	2.074- Lasing From Ho <sup>3+</sup> -Doped Fluorotellurite Microstructured Fibers Pumped by a 1120-nm Laser. IEEE Photonics Technology Letters, 2016, 28, 1084-1087.	2.5	8
46	Holmium-doped fluorotellurite microstructured fibers for 21  μm lasing. Optics Letters, 2015, 40, 469	5. 3.3	53
47	Synthesis of ultra-small BaLuF <sub>5</sub> :Yb <sup>3+</sup> ,Er <sup>3+</sup> @BaLuF <sub>5</sub> :Yb <sup>3+</sup> active-core–active-shell nanoparticles with enhanced up-conversion and down-conversion luminescence by a layer-by-layer strategy. Journal of Materials Chemistry C, 2015, 3, 2045-2053.	5.5	36
48	Dual mode emission of core–shell rare earth nanoparticles for fluorescence encoding. Journal of Materials Chemistry C, 2015, 3, 6314-6321.	5.5	24
49	Passively mode-locked fiber lasers at 1039 and 1560 nm based on a common gold nanorod saturable absorber. Optical Materials Express, 2015, 5, 794.	3.0	47
50	KMnF <sub>3</sub> :Yb <sup>3+</sup> ,Er <sup>3+</sup> @KMnF <sub>3</sub> :Yb <sup>3+</sup> active-core–active-shell nanoparticles with enhanced red up-conversion fluorescence for polymer-based waveguide amplifiers operating at 650 nm. Journal of Materials Chemistry C, 2015, 3, 9827-9832.	5.5	38
51	Flying upconversion fluorescent particles and direct observation of energy transfer and depopulation processes. CrystEngComm, 2015, 17, 587-591.	2.6	1
52	Growth of hexagonal phase sodium rare earth tetrafluorides induced by heterogeneous cubic phase core. RSC Advances, 2014, 4, 13490.	3.6	11
53	Controlled synthesis of ultrasmall hexagonal NaTm0.02Lu0.98â <sup>-,</sup> xYbxF4 nanocrystals with enhanced upconversion luminescence. Journal of Materials Chemistry C, 2014, 2, 2037.	5.5	43
54	Passively Q-switched erbium-doped fiber laser based on gold nanorods. Optik, 2014, 125, 5789-5793.	2.9	17

#	Article	IF	CITATIONS
55	Sub-10 nm BaYF5:Yb3+,Er3+ core–shell nanoparticles with intense 1.53 μm fluorescence for polymer-based waveguide amplifiers. Journal of Materials Chemistry C, 2013, 1, 1525.	5.5	50
56	Enhanced deep-ultraviolet upconversion emission of Gd3+ sensitized by Yb3+ and Ho3+ in β-NaLuF4 microcrystals under 980 nm excitation. Journal of Materials Chemistry C, 2013, 1, 2485.	5.5	72
57	Gold nanorods as saturable absorbers for all-fiber passively Q-switched erbium-doped fiber laser. Optical Materials Express, 2013, 3, 1986.	3.0	105
58	Broadband amplification and highly efficient lasing in erbium-doped tellurite microstructured fibers. Optics Letters, 2013, 38, 1049.	3.3	17
59	Passively mode-locking induced by gold nanorods in erbium-doped fiber lasers. Applied Physics Letters, 2013, 103, .	3.3	119
60	Citric acid-assisted hydrothermal synthesis of α-NaYF4:Yb3+,Tm3+ nanocrystals and their enhanced ultraviolet upconversion emissions. CrystEngComm, 2012, 14, 2302.	2.6	48
61	Passively Q-switching induced by gold nanocrystals. Applied Physics Letters, 2012, 101, .	3.3	122
62	Greatly enhanced size-tunable ultraviolet upconversion luminescence of monodisperse β-NaYF4:Yb,Tm nanocrystals. Journal of Materials Chemistry, 2011, 21, 13413.	6.7	82
63	Widely tunable passively mode-locked fiber laser with carbon nanotube films. Optical Review, 2010, 17, 97-99.	2.0	12